I-1. PROJECT RESEARCHES

Project 7

PR7 Project Research on Advances in Isotope-Specific Studies Using Muti-Element Mössbauer Spectroscopy

M. Seto

Institute for Integrated Radiation and Nuclear Science, Kyoto University

OBJECTIVES OF RESEARCH PROJECT:

One of the most irreplaceable features of the Mössbauer spectroscopy is to extract several information such as electronic states for a specific isotope. The main objectives of this project research are the investigation in the frontier of the materials science and the development of advanced experimental methods by using multi-element Mössbauer spectroscopy. Promotion of variety of Mössbauer isotope provides more useful and valuable methods in modern materials science even for complicated systems.

In this project research, each group performed their research by specific isotopes:

^{57}Fe in P7-1, P7-2, P7-3, P7-4, P7-5, P7-9, and P7-13

^{61}Ni in P7-8

^{119}Sn in P2-5, P7-7 and P7-10

^{151}Eu in P2-5, P7-9, P7-10 and P7-11

^{197}Au in P7-6 and P7-7

Other isotopes in P7-11 and P7-12

MAIN SUBJECTS AND RESULTS OF THIS REPORT:

Main subjects and results from these researches are as follows:

(P7-1, K. Shinoda) Intensity Tensor of Fe^{2+} in the *M2* Site of Hypersthene by Single Crystal Mössbauer Microspectroscopy

K. Shinoda *et al.* characterized the electric field gradient tensor of single crystals of hypersthene as small as 1mm^3 by developed Mössbauer microspectrometer.

(P7-2, H. Fujii) Mössbauer Study of the Model Complexes of Heme Enzymes

H. Fujii *et al.* investigated model complexes of cytochrome P450 in different solvents of acetonitrile, tetrahydrofuran and methanol to obtain comparable results from the EPR experiments.

(P7-3, Y. Akiyama) Analysis of Iron-based Products Using Mössbauer Spectroscopy - Iron Oxide Scale Generated in the Boiler Feed-water in Thermal Power Plant -

Y. Akiyama *et al.* are investigating a design for the magnetic separation system of the iron oxide scale from power plant through evaluation of ferromagnetic and paramagnetic components.

(P7-4, I. Mashino) Electrical Conductivity and the Iron Valence State of Enstatite Glasses up to Mbar Pressures

I. Mashino *et al.* investigated pressure dependence of electrical conductivity of Fe-bearing enstatite glasses. The Mössbauer spectroscopy is used to determine the composition ratio of Fe^{2+} and Fe^{3+}components.

(P7-5, Y. Matsushi) The Role of Iron in the Differential Weathering Processes of Volcanic Fall Deposit

H. Fukui *et al.* investigated several soil samples with different weathering patten to reveal the crucial role of iron in the weathering process.

(P7-6, H. Ohashi) Rough Estimation of Debye Temperature for Precursor of Supported Gold Cluster Catalysts Derived from Recoil-Free Fraction in ^{197}Au Mössbauer Spectroscopy

H. Ohashi *et al*. investigated Au_2S_x, a precursor of supported Au cluster and evaluated its Debye temperature, which was quite low but appropriate as Au catalysts.

(P7-7, Y. Kobayashi) Recoilless Fraction on ^{197}Au Mössbauer Spectroscopy

Y. Kobayashi has investigated the evaluation method of the Debye temperature for Au compounds.

(P7-8, T. Kitazawa) ^{61}Ni Mössbauer Spectroscopy for Supramolecular Bridging Cyanide Complexes

T. Kitazawa *et al*. have investigated several Ni cyanides to evaluate slight difference of Ni environments.

(P7-9, H. Wadachi) Mössbauer Spectroscopy of a Perovskite-Type Iron Oxide $Ba_{2/3}La_{1/3}FeO_3$

M. Onose *et al*. have revealed the temperature dependence of Mössbauer spectra of $Ba_{2/3}La_{1/3}FeO_3$ to find the magnetic structure of spin charge ordering.

(P7-10, Y. Kamihara) Research on Magnetism in a Novel Kondo Lattice III

Y. Kamihara *et al*. studied the temperature dependence of $EuSn_2P_2$ by using both ^{151}Eu and ^{119}Sn Mössbauer spectroscopy to elucidate its magnetic ordering.

(P7-11, R. Masuda) Optimization for the Energy Standard Material for Mössbauer Spectroscopy

R. Masuda *et al*. evaluated the efficiency of a standard material for Mössbauer spectroscopy using EuF_3.

(P7-12, S. Kitao) Development of ^{180}Hf Mössbauer Spectroscopy

S. Kitao *et al*. have attempted to observe ^{180}Hf Mössbauer spectra using a HfC source material.

(P7-13, K. Yonezu) Experimental Preliminary Approach on the Precipitation Mechanism of Banded Iron Formation (BIF)

K. Yonezu *et al.* are investigating sedimentary rock to understand its formation mechanism.

PR7-1 Intensity tensor of Fe^{2+} in the *M*2 site of hypersthene by single crystal Mössbauer microspec-troscopy

K. Shinoda[1], K. Onoue[1], Y. Kobayashi[2]

[1]*Department of Geosciences, Graduate School of Science, Osaka Metropolitan University*
[2]*Institute for Integrated Radiation and Nuclear Science, Kyoto University*

INTRODUCTION: Pyroxene is a major rock-forming mineral and a typical multi-site solid solution. Common chemical formula of natural pyroxene is $(Ca, Fe, Mg)_2 Si_2 O_6$. Occupying sites of divalent cations are the *M*1 and *M*2 sites. In pyroxene, Fe^{2+} in *M*1, Fe^{2+} in *M*2 and Fe^{3+} in *M*1 sites are possible. Fe^{2+} in the *M*1 site shows a little wider quadrupole doublet than Fe^{2+} in the *M*2 site in Mössbauer spectra. Fe^{3+} in the *M*1 site shows the narrower quadrupole doublet than Fe^{2+}. Intensities of component peaks in a quadrupole doublet of a thin section as a single crystal are asymmetric and vary depending on the angle between the direction of incident γ-rays and the crystallographic orientation of the thin section. Intensity of quadrupole doublet (I^h / I^{total}) means a ratio between area of the peak of the higher energy (I^h) and total area of the doublet ($I^{total}= I^h + I^l$) (sum of I^h and area of the lower energy (I^l)). In tensity of quadrupole doublet can be calculated from the intensity tensor. In Mössbauer spectrum of pyroxene in which three doublets are overlapping, it is important to know intensity tensors of the three doublets to separate overlapping doublets. Zimmermann (1975, 1983) showed relationships between the intensity tensor and electric field gradient (EFG) tensor and introduced experimental determination of the intensity tensor from the Mössbauer spectrum of a single crystal. Shinoda and Kobayashi (2019) revealed EFG tensor due to Fe^{2+} in *M*2 site of ortho-enstatite, which is orthorhombic Fe-poor pyroxene of chemical formula $(Mg_{2.03}, Fe_{0.16})$ $(Si_{1.78}, Al_{0.13})$ O_6. However, the intensity tensor of Fe-rich orthopyroxene has not been revealed. In this study, the intensity tensor of Fe^{2+} at the *M*2 site of hypersthene $(Ca_{0.06}, Mg_{1.26}, Fe_{0.68})$ $(Si_{1.95}, Al_{0.05})$ O_6 by EDS analyses were determined by single crystal ^{57}Fe Mössbauer spectra using crystallographically oriented thin sections.

EXPERIMENTS and RESULTS: Single crystals of hypersthene as small as $1mm^3$ from Inawashiro-ko, Aizu-wakamatsu, Fukushima, Japan were used for this study. Three crystallographically oriented thin sections perpendicular to ***a****, ***b**** and ***c**** were prepared by measuring X-ray diffraction using Laue and precession camera. Seven Mössabuer spectra of oriented thin sections were measured. In this study, Cartesian coordinate (*X Y Z*) is set as *X*//***c****, *Y*//***a****, *Z*//***b****, where ***a****, ***b****, ***c**** are reciprocal lattice vectors of hypersthene. Mössbauer measurements were carried out in transmission mode on a constant acceleration spectrometer with an Si-PIN semiconductor detector (XR-100CR, AMPTEK Inc.) and multi-channel analyzer of 1024 channels. A 3.7GBq ^{57}Co/Rh of 4mmϕ in diameter was used as γ-ray source. An ^{57}Fe-enriched iron foil was used as velocity calibrant. The two symmetric spectra were folded and velocity range was ±4mm/s. Thickness corrections of raw spectra were not done.

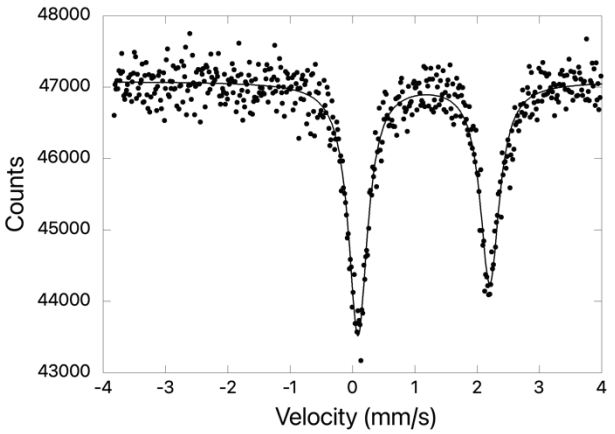

Fig.1 Mössbauer spectrum of hypersthene measured under γ-ray parallel to the ***a****-axis.

Fig.1 shows Mössbauer specrtum of hypersthene measured under incident γ-ray parallel to ***a****-axis. A doublet due to Fe^{2+} in *M*2 site of hypersthene was observed. Averages of isomer shift, Q-splitting, and line width were 1.15 2.13 and 0.39 mm/s, respectively. From seven sets of intensity of quadrupole doublet, three components (I_{XX}, I_{YY}, and I_{ZZ}) of the intensity tensor of Fe^{2+} in the *M*2 site of hypersthene are obtained as 0.577, 0.453 and 0.470. three components of the intensity tensor of Fe^{2+} in the *M*2 site of ortho-enstatite were 0.615, 0.455 and 0.424 (Shinoda and Kobayashi, 2019). Three components of the intensity tensor of Fe-poor and Fe-rich ortho-pyroxene suggest that I_{XX} and I_{ZZ} show weak chemical dependence of Fe^{2+} and I_{YY} is independent of Fe^{2+} components.

REFERENCES

[1] Zimmermann, R. (1983) Advances in Mössbauer spectroscopy (Thosar, B.V. Ed.). pp.273-315, Elsevier Sci-entific Publishing Co. Amsterdam.
[2] Zimmermann, R. (1975) Nucl. Instr. and Meth. **128**, 537-543.
[3] Shinoda and Kobayashi (2019) KURNS Progress Report 2019.

PR7-2 Mössbauer Study of the Model Complexes of Heme Enzymes

H. Fujii, Y. Kobayashi[1], A. Takeda, S. Iwamoto

Graduate School of Science, Nara Women's University
[1]Graduate School of Science, Kyoto University

INTRODUCTION: Iron porphyrin complexes are active sites of many heme proteins in nature. For example, cytochrome P450 generates a high-valent oxoiron(IV) porphyrin π-cation radical species called compound I in the catalytic cycle. The oxidation state and the spin state of the compound I are key for controlling the function of tcytochrome P450. In this project, we prepared a model complex (FeS) of cytochrome P450 and studied the oxidation state and the spin state of FeS by using Mössbauer spectroscopy.

EXPERIMENTS: Mössbauer spectroscopy was conducted in conventional transmission geometry by using ^{57}Co-in-Rh(50 mCi) as γ-ray source. The Doppler velocity scale was calibrated using an Fe metal foil at room temperature. ^{57}Fe was purchased from commercial as a powder and changed to iron(II) acetate. Synthesis of FeS and its iron(III) chloride complex will be reported in elsewhere.

RESULTS: EPR spectra of FeS indicated that FeS is a mixture of ferric high spin state and ferric low spin state in acetonitrile (AC) at 4K while FeS is a ferric low spin complex in tetrahydrofuran (THF) and methanol. These results can be interpreted by the coordination of THF and methanol, which work as oxygen donor ligand for the heme iron, in THF and methanol, respectively. The binding of THF or methanol is consistent to the coordination of water ligand in cytochrome P450. To confirm the change of the spin state of FeS with coordination of these solvent ligand, we measured Mössbauer spectra of FeS in AC, THF, and methanol at 6K (Figure 1). Mössbauer parameters are listed in Table 1. We found that the Mössbauer peaks from all of these samples are extremely broad, compared with those of other ferric porphyrin complexes. This is also close to the nature of cytochrome P450, for which extremely broad Mössbauer peaks have been reported. These results suggest that FeS can mimic the active site of cytochrome P450. We found two Mössbauer peaks in AC, but one peak in THF and methanol. We tentatively assigned these peaks on the basis of the EPR results. The two peaks in AC result from high spin state and low spin state of FeS; the peak around 0 mm/s results from high spin state and the peak around 1.5 mm/s results from low spin state. On the other hand, the peaks in THF and methanol are assignable to the low spin state. These assignments were further supported by Mössbauer spectrum in AC at 77 K.

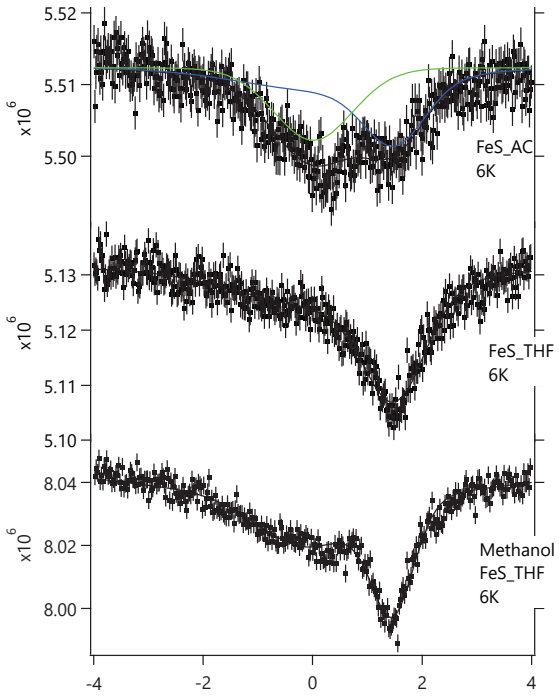

Fig 1. Mössbauer spectra (6 K) of FeS in acetonitrile (top), in THF (middle), and in methanol (bottom).

Table 1. Mössbauer parameters of FeS at 6 K.

	Ratio	IS	QS	FWHM1	FWHM2
AC	57.0%	0.891	1.213	3.658	1.209
	43.0%	0.011		1.607	
THF		0.891	1.213	3.658	1.209
methanol_THF		0.674	1.575	2.041	0.824

REFERENCES:

[1] H. Fujii, in *Heme Peroxidases*,edited by E. Ravan, and B. Dunford (The Royal Society of Chemistry: London, 2016), pp 183-217.
[2] M. Sharrock *et al.*, Biochemistry, **12** (1973) 258-265.
[3] P. G. Debrunner *et al.*, Proc. Natl. Acad. Sci., 93 (1996) 12791-12798.

PR7-3 Analysis of Iron-based Products Using Mössbauer Spectroscopy - Iron Oxide Scale Generated in the Boiler Feed-water in Thermal Power Plant -

Y. Akiyama, M. Okumura, K. F. Mishima[1], S. Nishijima[1], H. Okada[2], N. Hirota[2], T. Yamaji[3], H. Matsuura[3], S. Namba[3], T. Sekine[4], Y. Kobayashi[5], M. Seto[5]

Graduate School of Engineering, Osaka University
[1] *Department of Nuclear Technology and Applied Engineering, Fukui University of Technology*
[2] *National Institute for Materials Science*
[3] *Shikoku Research Institute Inc.,*
[4] *Ebara Industrial Cleaning Co., Ltd.,*
[5] *Institute for Integrated Radiation and Nuclear Science, Kyoto University*

INTRODUCTION: The power generation efficiency of thermal power plants decreases due to corrosion products (iron oxide scale) formed in the feed-water system. In this study, removal of iron oxide scale from thermal power plants applying oxygen treatment (OT) using high gradient magnetic separation (HGMS) was investigated.

While the scale of thermal power plants applying all volatile treatment (AVT) is mainly composed of ferromagnetic particles, the OT scale is mainly composed of paramagnetic particles, which are difficult to capture by magnetic force. Our previous analysis of the scale collected from actual OT-adopted thermal power plant using Mössbauer spectroscopy showed that the OT scale contains up to 20% ferromagnetic particles, while the other components are paramagnetic particles, and these particles do not form co-crystal [1].

Based on the results, we proposed the two-stage magnetic separation system shown in Fig.1, that captures ferromagnetic particles in the first stage and paramagnetic particles in the second stage [2]. To design the magnetic separation system for an actual thermal power plant used at high temperature, we focused on the second stage and investigated the change in the capture performance of paramagnetic scale by the temperature.

EXPERIMENTS: High-gradient magnetic separation using superconducting solenoidal magnet was conducted targeting hematite (Fe_2O_3), which is the main component of OT scale. Suspension of 20.0 g of hematite particles at 500 ppm was prepared, and the experiment was conducted at 25-80 °C under the conditions of magnetic field of 6 T, flow velocity of 20 cm/s, and pH=4. These conditions assume the installation of separation equipment in the chemical cleaning line of a thermal power plant boiler feedwater system. The filters made of ferromagnetic stainless steel were installed inside the superconducting magnet. In case the fluid passing through the superconducting magnet was hot, cooling water was flowed between the magnet and the piping to prevent the magnet from temperature increasing. The results were compared with simulations based on particle trajectory calculations based on the magnetic field and flow velocity distributions around the ferromagnetic filter wire.

RESULTS: Fig. 2 shows the captured amount for each of the five filters. The captured amount increased as the temperature increased. In comparison with the simulation results, the measured value was lower than the estimated value, and the difference tended to increase as the temperature increased [3]. The reason is thought to be the increase in thermal motion of hematite particles and the decrease in fluid temperature due to the cooling water in the magnetic separation section. Based on this, the captured amount was re-calculated considering these effects. As a result, it was estimated that 90 % of the generated paramagnetic particles could be captured by installing 2745 filters in the practical scale. Based on the results, we were able to design the magnetic separation system and conditions for the introduction of a two-stage magnetic separation system for the practical use.

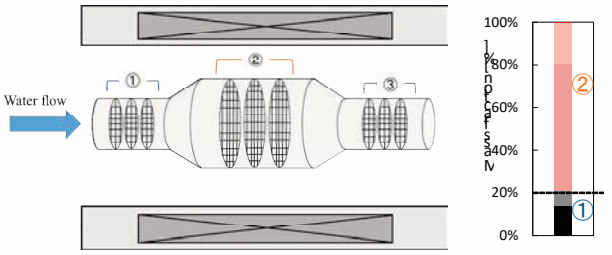

Fig.1 Composition of the scale collected at low-pressure heater drain measured by the Mössbauer spectroscopy and the two-stage magnetic separation system. based on it.

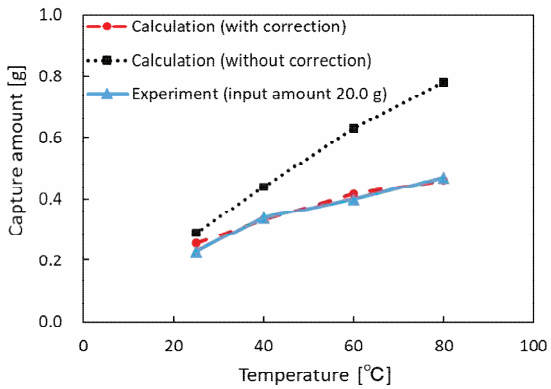

Fig.1 Temperature dependence of capture amount of hematite per a filter.

REFERENCES:

[1] M. Hiramatsu *et al.,* J. Phys. Conf. Ser., 1293 (2019) 012079.
[2] K. Akiyama *et al.*, IEEE Transactions on Applied Superconductivity, Vol. 31, No. 5, (2021) 3700204.
[3] M. Okumura, *et al.*, IEEE Transactions on Applied Superconductivity, in press.

PR7-4 Electrical conductivity and the iron valence state of enstatite glasses up to Mbar pressures

I. Mashino, T. Yoshino, S. Kitao[1], T. Mitsui[2], R. Masuda[3]

Institute for Planetary Materials, Okayama University
[1]Institute for Integrated Radiation and Nuclear Science, Kyoto University
[2]Synchrotron Radiation Research Center, Kansai Photon Science Institute, Quantum Beam Science Research Directorate, National Institutes for Quantum and Radiological Science and Technology
[3]Graduate School of Science and Technology, Hirosaki University

INTRODUCTION: The existance of gravitationally stabilized melts at the bottom of the Earth's mantle has been proposed because a density crossover between melts and crystals is expected to occur. However, whether the crossover occurs in the lower mantle or not strongly depends on the chemical composition of both the melt and crystals. The valence and spin states of iron are believed to affect the iron partitioning between melts and crystals, thus also control a depth of the density crossover [1]. In order to understand the valence/spin states of iron in silicate melts, we firstly conducted high-pressure electrical conductivity measurements of iron-bearing enstatite glass which has a representative composition of the mantle, because silicate glasses have been considered as good analogues of silicate melts.

EXPERIMENTS: ^{57}Fe-bearing enstatite glasses (hereafter Fe-enstatite glass) were synthesized from reagent MgO, $^{57}Fe_2O_3$ and SiO_2 powders. The mixtures of oxides were placed in a platinum crucible and melted at 1650 °C, and subsequently quenched by immersing the base of the crucible in water. The conventional ^{57}Fe-Mössbauer spectroscopy was performed using a ^{57}Co source in Rh matrix with nominal activity of 1.85 GBq at Institute for Integrated Radiation and Nuclear Science, Kyoto University. The velocity scale is referenced to α-Fe. According to the Mössbauer spectroscopy, iron in the synthesized glasses was found to be present as shown in Table 1. Compared with hyperfine parameters in silicate glasses previously reported at ambient condition [2, 3], doublet 1 and doublet 2 can be associated with Fe^{3+} and Fe^{2+} in octahedral site, respectively.

Table 1.
Fitting results of the ambient conventional Mössbauer spectra of Fe-enstatite glasses

Doublet 1 (Fe^{3+})			Doublet 2 (Fe^{2+})		
CS (mm/s)	QS (mm/s)	Aria ratio (%)	CS (mm/s)	QS (mm/s)	Aria ratio (%)
13 mol% Fe-bearing enstatite glass					
0.36	1.27	57	1.04	1.98	43
19 mol% Fe-bearing enstatite glass					
0.34	1.25	65.2	1.05	2.01	34.8
10 mol% Fe, 10 mol% Al-bearing enstatite glass					
0.34	1.24	43	1.03	1.91	57

The synthesized glasses were loaded into a diamond anvil cell with 150 and 300 μm culets. The gold foils electrically insulated by Al_2O_3 layer were attached to the sample and connected to platinum electrodes outside the sample hole. Electrical conductivity measurements were performed at Institute for Planetary Materials, Okayama University using the two-wire terminal method with an alternating current signal, an amplitude of 1 V and within a frequency range of 0.1–1 MHz.

RESULTS: Fig. 1 shows the obtained electrical conductivity of Fe-enstatite glasses with various iron contents as a function of pressure at 300 K in this study. At lower pressure, the electrical conductivity of Fe-enstatite glasses gradually increases with increasing pressure. At pressures above 70 GPa, the conductivity decreases once and then increases in higher pressure (shadowed areas in Fig. 1). Previous studies observed the trend change in electrical conductivity of (Mg,Fe)O ferropericlase between 25 and 40 GPa, which is likely associated with spin transition from high-spin to low-spin states of iron [4, 5]. The trend change in Fe-enstatite glasses is similar to the previous results. Therefore, the spin transition of iron is one possibility to account for the trend change. Another possibility is that $Fe^{3+}/\Sigma Fe$ ratio changes under high pressure. In previous Mössbauer spectroscopic study of Na, Fe-bearing silicate glass, the $Fe^{3+}/\Sigma Fe$ slightly increases around 60 GPa [6]. Generally, the electrical conductivity changes depending on $Fe^{3+}/\Sigma Fe$ ratio. The trend change can be also explained by the change of $Fe^{3+}/\Sigma Fe$ ratio with increasing pressure. Besides the ambient conventional Mössbauer data, a high-pressure synchrotron Mössbauer spectroscopic experiment was performed for the enstatite glass with 13 mol% Fe. Geophysical discussion is now ongoing.

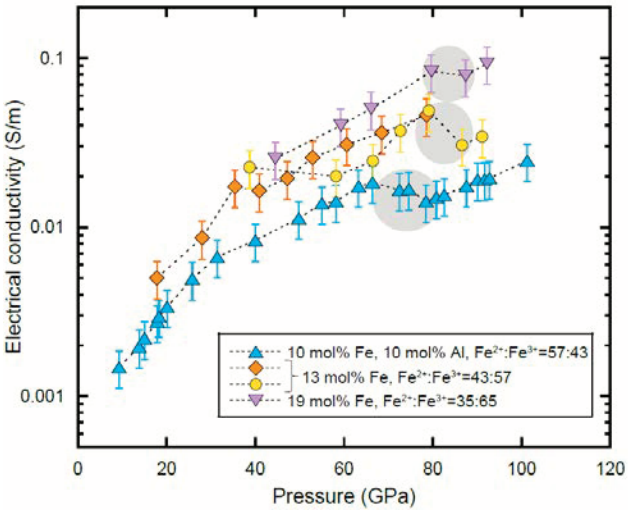

Fig. 1. Electrical conductivities of Fe-bearing enstatite glasses as a function of pressure at 300 K.

REFERENCES:

[1] R. Nomura *et al.*, Nature **473**, 199 (2011).
[2] M. Dyar, Am. Mineral. **70**, 304 (1985).
[3] B. Mysen and P. Richet, *Silicate Glasses and Melts* (Elsevier, 2019).
[4] K. Ohta *et al.*, Proc. Japan Acad. Ser. B **83**, 97 (2007).
[5] T. Yoshino *et al.*, J. Geophys. Res. **116**, 1 (2011).
[6] C. Prescher *et al.*, Earth Planet. Sci. Lett. **385**, 130 (2014).

PR7-5 The role of iron in the differential weathering processes of volcanic fall deposit

H. Fukui, Y. Matsushi[1], S. Kitao[2], Y. Kobayashi[2], K. Shinoda[3], T. Watanabe[4]

Graduate School of Science, Kyoto University
[1]Disastert Prevention Research Institute, Kyoto University
[2]Institute for Integrated Radiation and Nuclear Science, Kyoto University
[3]Graduate School of Science, Osaka city University
[4]Graduate School of Agriculture, Kyoto University

INTRODUCTION: During the alteration of volcanic material into secondary mineral, iron plays an important role. Iron is easy to precipitate under an oxidizing condition, whereas under a relatively reducing condition, because the divalent cation is present in liquid phase, it could contribute to the formation of aluminosilicate [1]. Moreover, halloysite, one of the clay minerals, could be easy to form under the condition in which ferrous iron is present [2]. The aim of the study is to evaluate the role of iron in the weathering processes of volcanic material by examining the chemical state using ^{57}Fe Mossbauer spectroscopic analysis.

EXPERIMENTS: We collected soil samples containing an Andesitic pumice, Ta-d2, at Atsuma town, southern part of Hokkaido, Northern Japan. The soil has altered into the three weathering pattern, reddish-weathered pumice (RP), white-weathered pumice (WP), and greyish-weathered pumice (GP) [3]. To examine the valence and chemical-bonding state of iron included in the soil, we conducted room-temperature (300 K) and cryogenic (22K) ^{57}Fe Mossbauer spectroscopic analysis. We measured Mossbauer spectra using ^{57}Co with Rh matrix as a radiation source for 6 representative powder samples. In addition to the powder samples, to examine the weathering condition within a single pumice, we conducted in-situ Mossbauer analysis for a thin section of the pumice using 0.5 mm diameter pinhole.

RESULTS AND DISSCUTIONS: Ferrous/ferric ratio in the representative powder samples at GP, RP and WP were shown in Fig. 1A. GP contained the largest amount of ferrous ion, 56.6%, whereas RP contained smaller amount and WP did the lowest amount of ferrous iron. Clay fraction obtained from WP sample had no divalent iron. Also, both S3-50 and S1-60 located at shallower part of Ta-d2 showed less amount of ferrous iron and more amount of ferric iron than both S3-80 and S1-80 located at deeper part of Ta-d2.

Fig. 1B indicates the ferrous/ferric ratio of 8 locations, P1 to P8, for in-situ pinhole Mossbauer analysis within a single pumice. The greyish cores of pumice, P4 and P6, have the highest amount of ferrous iron, whose values were similar to the powder sample of GP (Fig. 1A). On the other hand, the white rind of pumice, P3 and P5, showed no ferrous iron, all of which have altered into trivalent state. On the reddish band located in between the core and rind, P1 and P2 have an intermediate content of ferrous ion. P6 located just inside the reddish band contained much larger amount of ferrous ion, whereas P7 and P8 just outside the reddish band contained no ferrous iron.

The results revealed that iron in the Ta-d2 pumice follow a different reaction path; under an oxidizing condition of RP, the pumice altered into iron (hydr)oxides such as goethite and hematite, whereas under a relatively reduced condition of WP and GP, halloysite could be easy to form because divalent iron would be present in the solution. Although iron takes trivalent state both in RP and WP, the value of QS (quadrupole splitting) was completely different, 0.75 mm/sec for RP and 0.58 mm/sec for WP, indicating that chemical-bonding state of iron plays a crucial role on the differential weathering of Ta-d2.

REFERENCES:

[1] Gainey *et al.*, Nat. Commun., **8** (2017) 1230.
[2] Churchman *et al*., Clay Miner., **51**(2016) 395-416.
[3] Fukui *et al*., Catena (in preparation).

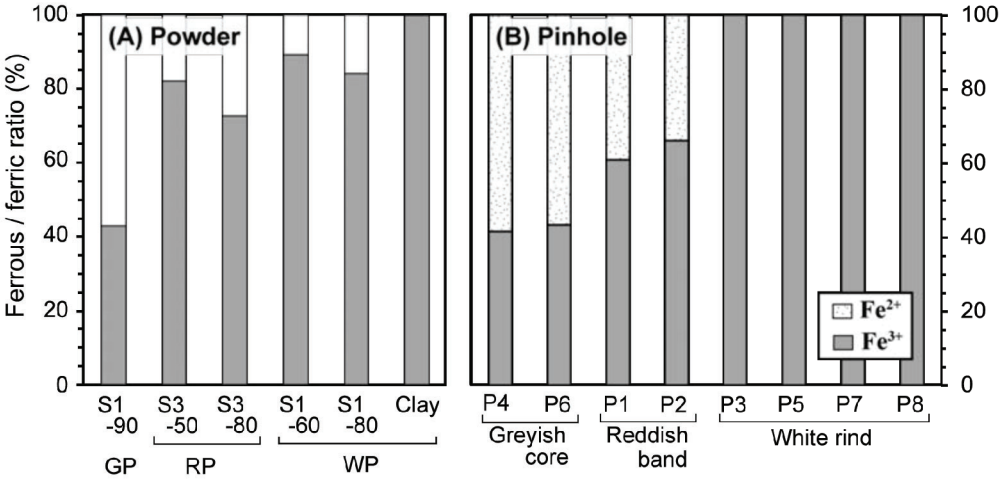

Fig. 1. Ferrous/ferric ratio of (A) 6 powder samples and (B) 8 in-situ Mossbauer analysis of a thin section. Sampling locations of powder samples (A) and position ID, P1 to P8 (B), are indicated in the referenced paper [3] in preparation.

PR7-6 Rough estimation of Debye temperature for precursor of supported gold cluster catalysts derived from Recoil-free fraction in ^{197}Au Mössbauer spectroscopy

H. Ohashi, T. Sai, R. Tawatari, K. Kikuchi, H. Murayama[1], T. Ishida[2], D. Kawamoto[3], Y. Kobayashi[4], S. Kitao[4]

Faculty of Symbiotic Systems Science, Fukushima University
[1]Faculty of Sciences, Kyushu University
[2]Department of Applied Chemistry for Environment, Tokyo Metropolitan University
[3]Faculty of Sciences, Okayama University of Science
[4]Institute for Integrated Radiation and Nuclear Science, Kyoto University

INTRODUCTION:

Though sulfide deposition-precipitation (SDP) method was a kind of new DP method, it was a very unique method and different from DP on several points such as preparation pH. However, until now, the structure of gold sulfide as a precursor synthesized by the SDP method was unknown.

On the other hand, Mössbauer effect (recoilless nuclear resonance) is the phenomenon of resonant absorption of γ-radiation, emitted at the radioactive decay of a nucleus in a radioactive material, which act as absorber. This method is widely used in material research that contains iron (^{57}Fe) and tin (^{119}Sn), which are easy to obtain radioactive isotopes that are radiation sources. However, ^{197}Au Mössbauer spectroscopy has not been widely used because radiation source, ^{197}Pt has short half-life.

The purpose of this study was to estimate the Debye temperature derived from recoil-free fraction in ^{197}Au Mössbauer spectroscopy for the precursor of heterogeneous gold catalysts by SDP method.

EXPERIMENTS:

Gold sulfide (Au_2S_x) and activated carbon supported gold sulfide were synthesized by the similar SDP method already reported[1]. ^{197}Au Mössbauer spectra were measured at Kyoto University Research Institute of Nuclear Science. The ^{197}Pt isotope ($T_{1/2}$ = 18.3 h), γ-ray source feeding the 77.3 keV Mössbauer transition of ^{197}Au, was prepared by neutron irradiation of isotopically enriched ^{196}Pt metal at the Kyoto University Reactor. The measurement temperature was 14 - 20 K, and the measurement was performed by the transmission method.

RESULTS:

The ^{197}Au Mössbauer spectra for gold foil (standard) and precursor of supported gold cluster catalysts were measured. These spectra were normalized by the content of gold (n) in measured sample. Each area (A) of normalized spectrum was calculated. There is a following relationship between recoil-free fraction (f) and area;

$$f = a\,A/n \quad \text{(eq.1)}$$

where "a" is proportional constant in this measurement equipment. On the other hand, equation of recoil-free fraction is as follows;

$$f = exp\left\{-\frac{6E_R}{k_B\theta_D}\left[\frac{1}{4}+\left(\frac{T}{\theta_D}\right)^2\int_0^{\frac{\theta_D}{T}}\frac{x\,dx}{e^x-1}\right]\right\} \quad \text{(eq.2)}$$

where k_B is Boltzmann constant, E_R is recoil energy, T is measurement temperature and θ_D is Debye temperature. Variations in the recoil-free fraction ($ln\ f$) of ^{197}Au Mössbauer spectrum as a function of Debye temperature derived from eq.2 were shown in Fig.1. Though Debye temperature for bulk gold was 165K, we estimated "a" in eq.1 from eq.2, and roughly estimated θ_D for the precursor from area and eq.2. It was turned out that $\theta_{D\text{-}precursor}$ was around 80 K. This θ_D was quite low but appropriate from the standpoint of precursor of gold cluster catalysts.

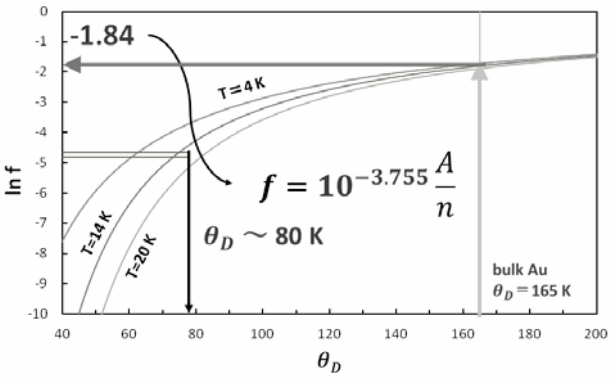

Fig.1. Variations in the recoil-free fraction ($ln\ f$) of ^{197}Au Mössbauer spectrum as a function of Debye temperature derived from eq.2.

REFERENCE:

[1] H. Ohashi *et al.*, "Method for dispersing and immobilizing gold fine particles and material obtained thereby", Patent No. 5010.

PR7-7 Recoilless Fraction on ^{197}Au Mossbauer Spectroscopy

Yasuhiro KOBAYASHI

Institute for Integrated Radiation and Nuclear Science, Kyoto University

INTRODUCTION: As a study of new materials, we are conducting Mössbauer spectroscopy of Au-supported catalysts. In the measurements, we noticed the samples in which the absorption intensity of the Mössbauer spectrum was small even though the amounts of Au in the samples were sufficient. This result indicates that the recoilless fraction is small, which is the probability of the Mössbauer absorption. In the case of nanoparticles, the recoilless fraction depends on the size of the particles. It could be the technique to measure the size of small nanoparticles that cannot be observed with an electron microscope.

Measuring the absolute amount of recoilless fraction is difficult due to the background fluctuations in the ^{197}Au Mössbauer measurement. Therefore, we investigated a method for estimating the Debye temperature from the temperature dependence of the spectral absorption intensity and confirmed its validity with pure Au foil.

The following equation describes the recoilless fraction f using the Debye model [1].

$$f = \exp\left[-\frac{3E_R}{2k\theta_D}\left\{1+4\left(\frac{T}{\theta_D}\right)^2 \int_0^{\theta_D/T} \frac{udu}{e^u-1}\right\}\right]$$

Here, T is the temperature, θ_D is the Debye temperature, and E_R is the recoil energy.

EXPERIMENTS: ^{197}Au Mössbauer measurement was conducted using a constant-acceleration spectrometer with a NaI scintillation counter. The ^{197}Au γ-ray source (77.3 keV) was obtained from ^{197}Pt (half-life; 18.3 hours) generated by irradiation of neutron to 98%-enriched ^{196}Pt metal foil using KUR. The γ-ray source and samples were cooled to the same temperatures using a helium refrigerator. The thickness of the Au foil (sample) was 20 μm. The isomer shift value of a gold foil was referenced to 0 mm/s.

RESULTS: Figure 1 shows the Mössbauer spectra at each temperature. The absorption areas on the spectra decrease at higher temperatures, indicating that the recoilless fraction decreases. Figure 2 shows the temperature dependence of the absorption area on the Mössbauer spectra. The areas are normalized by the value at 20K. The solid line is the calculated value from the equation. The absorption areas are proportional to the product of the recoilless fraction of the γ-ray source and the absorber. The Debye temperature of the γ-ray source is 270K, which is the Debye temperature of platinum metal. And the Debye temperature of the absorber is 164K from gold metal.

The observed absorption areas are in good agreement with the calculated curves. The observed area and the calculated value are normalized by the value of 20K, and no other corrections are made.

From this result, we found that the measurements of the temperature dependence of the absorption area are adequate for measuring the Debye temperature of the sample and are also helpful for the study of nanoparticles. In the future, we plan to measure temperature changes in various samples.

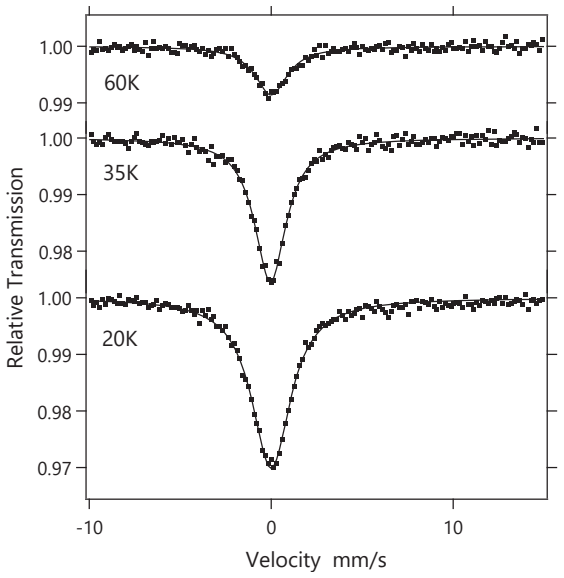

Fig. 1 The ^{197}Au Mössbauer spectra of Au foil at various temperatures.

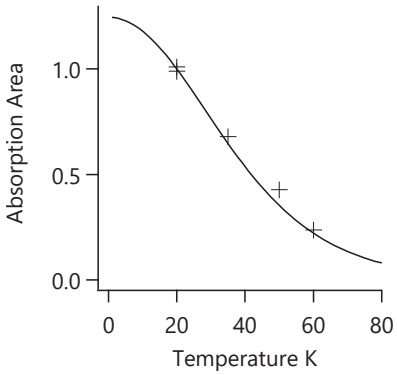

Fig. 2 Temperature dependence of the absorption area on the Mössbauer spectra. The markers are the observed absorption areas (normalized by the value at 20K), and the solid line is the calculated value.

REFERENCES:

[1] Gunther K. Wertheim, *Mössbauer Effect: Principles and Applications* (Academic Press, New York,1964).

PR7-8 ^{61}Ni Mössbauer Spectroscopy for Supramolecular Bridging Cyanide Complexes

Takafumi KITAZAWA[1,2], Kosuke KITASE1, Daiki UEDA[1], Daichi FUJIMOTO[1], Shunsuke ARAI[1], Yasuhiro KOBAYASHI[3], Shinji KITAO[3], Takumi KUBOTA[4] and Makoto SETO[3]

[1]*Faculty of Science, Toho University*
[2]*Research Centre for Materials with Integrated Properties, Toho University*
[3]*Institute for Integrated Radiation and Nuclear Science, Kyoto University*
[4]*Agency for Health, Safety and Environment, Kyoto University*

INTRODUCTION: The Mössbauer Effect has been found for about 100 nuclear transitions in some 80 nuclides in nearly fifty elements. The technique is a very valuable and helpful tool to the material sciences linking to molecular magnetisms. It is well-known that 3-d block transition metal complexes with d^4-d^7 configuration in an octahedral crystal field have a possibility of SCO between the low spin (LS) and the high spin (HS) state. Octahedral iron(II) SCO systems with $3d^6$ can be transited between the diamagnetic $(t_{2g})^6$ and the paramagnetic $(t_{2g})^4(e_g)^2$ configuration. Coordination polymers with bistable systems between the LS and the HS states, usually triggered by external stimuli, such as temperature, light, pressure and guest molecules, are a class of potential candidates for smart materials. As the very important history of SCO researches of the Hofmann-like coordination polymers, the SCO in Fe^{II}(pyridine)$_2$Ni(CN)$_4$ was found using ^{57}Fe Mössbauer spectroscopy and SQUID measurements in 1996 [1], SCO supramolecular Hofmann-like metal-organic frameworks containing 2D layers and 3D structures, with octahedral iron(II) ions linked by cyanidemetallates along the in-plane directions, have been investigated thoroughly for the development of interesting SCO materials in order to obtain potential applications in smart materials [2-7]. Ni(II) ions states are associated with Fe(II) ions state. Now we have carried out ^{61}Ni Mössbauer spectroscopy for three Hofmann type SCO compounds which act as different spin transition temperatures and behaviors including LS spin and HS spin ratios; Fe(pyridine)$_2$Ni(CN)$_4$, Fe(3-Methyl-py)$_2$Ni(CN)$_4$, and Fe(3-Cl-py)$_2$Ni(CN)$_4$, and mononuclear K_2[Ni(CN)$_4$].

EXPERIMENTS: We freshly synthesized Fe(pyridine)$_2$Ni(CN)$_4$, Fe(3-Methyl-py)$_2$Ni(CN)$_4$, and Fe(3-Cl-py)$_2$Ni(CN)$_4$, according to the applied methods [1,5-7] and mononuclear K_2[Ni(CN)$_4$].

^{61}Ni Mössbauer source production associated with ^{62}Ni(γ, p)^{61}Co was done using activation with Bremsstrahlung from the Electron beam of the KURNS-LINAC. ^{61}Ni Mössbauer measurements were carried out conventional methods, Since the half-life of ^{61}Co is about100 minutes, about three hours measurements were done for one cycle. For one SCO compound sample, three times cycles are carried out in order to get suitable Mossbaer spectra. All spectra were obtained at 16 K. Ni-14at%V alloy was used for characterizations of velocities.

RESULTS: As shown in Fig. 1, ^{61}Ni Mössbauer spectra of three SCO compounds with MOF(Metal Organic Framework) were found for the first time at 16K.

The obtained Mössbauer parameters have relationship with the square planar crystal field of $[Ni(CN)_4]_{2-}$ units. The parameters for three SCO compounds are slightly different due to slightly different Ni(II) environments, indicating environments of Ni(II) ions are associated with those of Fe(II) ions.

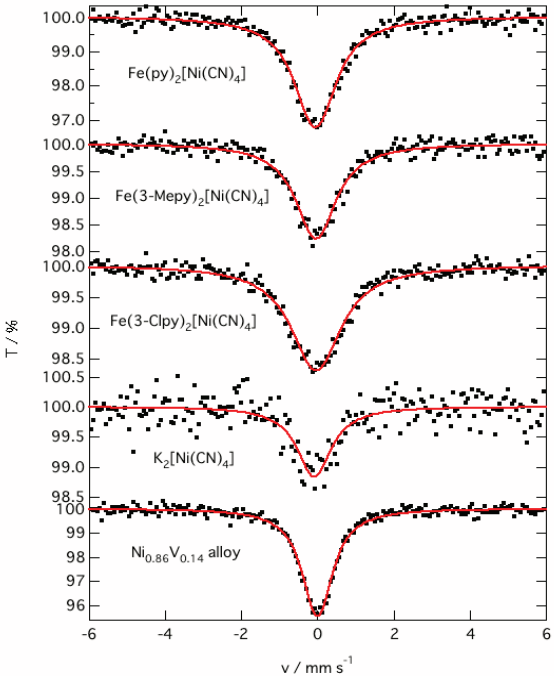

Fig.1 ^{61}Ni Mössbauer Spectroscopy for Supramolecular Bridging Cyanide Complexes.

REFERENCES:

[1] T. Kitazawa, Y. Gomi, M. Takahashi, M. Takeda, M. Enomoto, A. Miyazaki, T. Enoki, *J. Mater. Chem.* 1996, 6(1) 119-121, DOI:10.1039/JM9960600119.

[2] T. Kitazawa, Synthesis and Applications of New Spin Crossover Compounds. *Crystals* **2019**, *9*(8), 382;, DOI:10.3390/cryst9080382.

[3] K. Kitase, D. Akahoshi and T. Kitazawa, Inorg. Chem., 60, 7, 4717–4722 (2021).

[4] K. Kitase T. Kitazawa,, Dalton. Trans., 49, 12210-12214 (2020). (Back Cover)

[5] M. Gábor, T. Guillon, N. Moussa, L.Rechignat, T. Kitazawa, M. Nardone, B. Azzedine, *Chem. Phys. Lett.* 2006, **423**(1-3), 152-156.

[6] Kitazawa, T.; Eguchi,M.; Takeda, M; T, *Mol. Cryst. Liq. Cryst. Sci Tech. A*, 2000, 341, 527-532 DOI:10.1080/10587250008026193.

[7] T. Kitazawa, Mi. Takahashi, Ma. Takahashi, M. Enomoto, A. Miyazaki, T. Enoki, M. Takeda , *J. Radio-anal. Nucl. Chem.* 1999, 239(2), 285-290. DOI:10.1007/BF02349498.

PR7-9 Mössbauer spectroscopy of a perovskite-type iron oxide $Ba_{2/3}La_{1/3}FeO_3$

M. Onose[1,2], H. Takahashi[1], R. Takahashi[3], H. Wadati[3,4], S. Kitao[5], M. Seto[5], and S. Ishiwata[1]

[1]*Division of Materials Physics, Graduate School of Engineering Science, Osaka University*
[2]*Department of Applied Physics, the University of Tokyo*
[3]*Department of Material Science, Graduate School of Science, University of Hyogo*
[4]Institute of Laser Engineering, Osaka University
[5]*Institute for Integrated Radiation and Nuclear Science, Kyoto University*

INTRODUCTION: Spin and charge ordering in transition-metal oxides manifests itself as an emergent collective phenomenon of strongly correlated electrons. For example, a perovskite-type iron oxide $Sr_{2/3}La_{1/3}FeO_3$ is known to show a characteristic spin-charge ordering (SCO) as shown in Fig. 1, where six-fold collinear spin ordering and three-fold charge ordering as $3Fe^{3.67+} \rightarrow 2Fe^{3+} + Fe^{5+}$ are coupled with each other[1,2]. This spin/charge ordering ranges from $x = 0$ to $x = 0.75$ in its Ba-substituted system $(Sr_{1-x}Ba_x)_{2/3}La_{1/3}FeO_3$, whereas our previous neutron diffraction experiments for $x = 1$ suggests a spin-charge decoupling: whereas the magnetic structure of the ground state remains to be the same as that of the SCO phase, an unexpected G-type AFM phase appears as the high-temperature phase. To further clarify the existence or absence of charge disproportionation for $x = 1$, we performed Mössbauer spectroscopy measurements.

EXPERIMENTS: A polycrystalline sample of $x = 1$ was obtained by high-pressure synthesis. The ^{57}Fe Mössbauer spectra were measured with a ^{57}Co source in Rh. The velocity was calibrated with α-Fe. Fits to the Mössbauer spectra were performed by the least-squares method assuming Lorentzian peaks.

RESULTS: As shown in Fig. 2, the spectra in the paramagnetic phase ($180K \leq T \leq 293$ K) can be well fitted by quadrupole-splitted doublets for $Fe^{3.67+}$, and those below 140 K by the superposition of two sextets corresponding to Fe^{3+} and Fe^{5+}, indicating the emergence of the SCO phase along with our previous neutron diffraction measurements. Although the spectra at $T = 160$ K in the G-AFM phase are significantly broadened making it difficult to obtain a satisfactory fitting, the asymmetric spectral shape, i.e., an asymmetric distribution of isomer shift, suggests the development of incoherent charge ordering or the slowing down of charge fluctuation as $3Fe^{3.67+} \rightleftarrows 2Fe^{3+} + Fe^{5+}$. The hyperfine field for $x = 1$ are comparable with the previous study of $x = 0$[3], implying that they share the same SCO phase as a ground state. On the other hand, isomer shift (IS) for $x = 1$ is systematically larger than that for $x = 0$ by about 0.01 mm/s. This difference in IS is most likely due to the change in the bonding state of Fe-O, considering the IS of the related Fe^{4+} compounds $SrFeO_3$[4] and $BaFeO_3$[5].

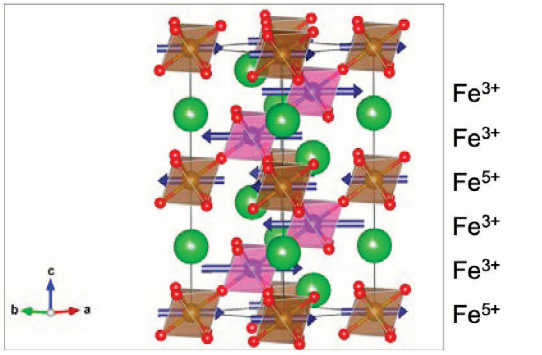

Fig. 1. Spin-charge ordered phase of $Sr_{2/3}La_{1/3}FeO_3$.

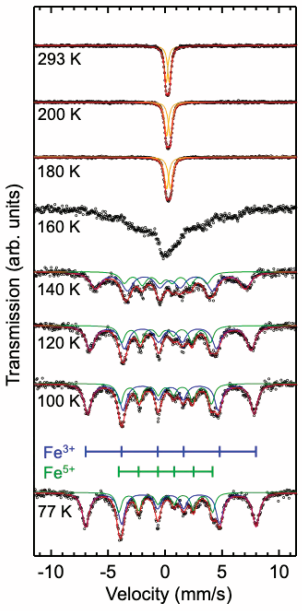

Fig. 2. Temperature dependence of the Mössbauer spectra for $Ba_{2/3}La_{1/3}FeO_3$ with the fitting curves of Lorentzian functions.

REFERENCES:

[1] P. D. Battle *et al*, J. Solid State Chem. **84**, 271 (1990).
[2] J. Q. Li *et al*, Phys. Rev. Lett. **79**, 297 (1997).
[3] J. Blasco *et al.*, Phys. Rev. B **98**, 104422 (2018).
[4] P. Adler *et al.*, Phys. Rev. B **73**, 094451 (2006).
[5] N. Hayashi *et al.*, Angew. Chem. Int. Ed. **50**, 12547 (2011).

PR7-10 Research on magnetism in a novel Kondo Lattice III

Y. Kamihara, Z. Liu, T. Shimura, S. Kitao[1], and M. Seto[1]

Department of Applied Physics and Physico-Informatics , Faculty of Science and Technology, Keio University

[1]Institute for Integrated Radiation and Nuclear Science, Kyoto University

The compounds with a 1:2:2 compositional ratio (so-called "122 compounds") are attractive for thermoelectric materials and topological conductor with spontaneous magnetic moments. [1-3] In 2018, high quality polycrystalline samples of $EuSn_2As_2$ have been reported using a new synthesis technique. [4, 5] In the report, we prepared a polycrystalline sample of $EuSn_2P_2$ according to the similar process to that of $EuSn_2As_2$. Theoretical magnetic phases of Eu sub lattice are calculated as ferromagnetic along to (*a*, *b*) axis and antiferromagnetic along to *c* axis. The magnetic phases are dominated by *s-f* interaction between Eu 4f electrons via itinerant electrons.

Gui *et al.* reported that a Neel temperature of the Eu sublattice was about 30 K in $EuSn_2P_2$. [2] In the polycrystalline sample, Gui *et al.* also reported that antiferromagnetic phase with spontaneous magnetic moments ~6 μ_B at 2 K under 5 tesla. The reported spontaneous magnetic moments were smaller than those of theoretical Eu^{2+} ions with spontaneous magnetic moments ~7 μ_B. A possible mechanism, which should explain the difference between experimental and theoretical magnetic moments of Eu^{2+}, is controversial. In this report, we demonstrate element-specific internal magnetic fields measurement for the polycrystalline $EuSn_2P_2$ using Mössbauer spectroscopy.

EXPERIMENTS: According to our previous report, polycrystalline samples of $EuSn_2P_2$ were prepared from Eu ingots and Sn-P pellets via a liquid phase reaction in carbon crucibles within evacuated silica tubes. [4] X-ray diffraction measurements at room temperature (RT) were performed in order to characterize the crystallographic phases of powdered sample of as-grown $EuSn_2P_2$. In this research, we have measured ^{151}Eu and ^{119}Sn Mössbauer spectra for polycrystalline $EuSn_2P_2$ using conventional optical setting. Both of ^{151}Eu and ^{119}Sn Mössbauer spectra demonstrates magnetic splitting at low temperatures. The spectra were fitted to Lorenzian line shapes using the MossWinn [6, 7] Program.

RESULTS: Figure 1 shows temperature dependence of ^{151}Eu Mössbauer spectra observed for our polycrystalline sample. At temperature (T) = 298 K, there are apparent two structures, which are due to the emission and absorption of the gamma ray in the sample.

The structures are assigned for two valent states of Eu ions in $EuSn_2P_2$; i.e. a mixed valent state of Eu ions. The mixed valent state is similar to that observed for Eu ions in $EuSn_2As_2$. [6]

At T = 15 K, a splitting of the lower structure is clearly observed. The splitting is mainly due to an existence of finite internal magnetic field.

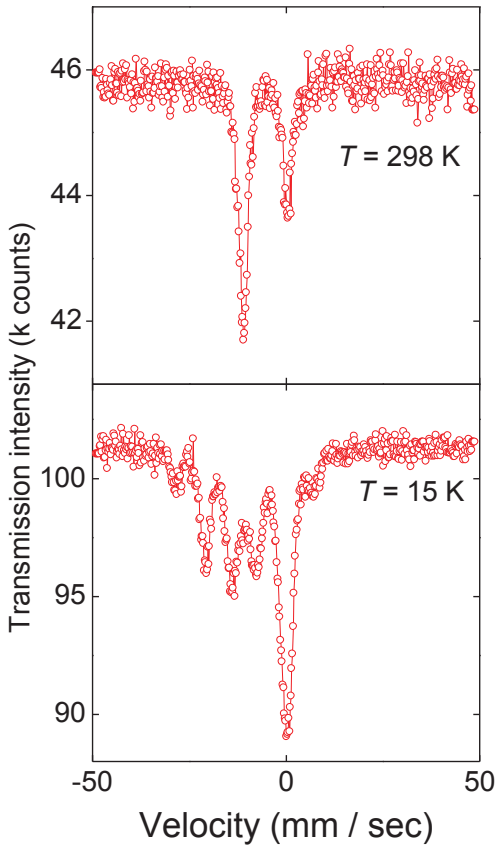

Fig. 1. ^{151}Eu Mössbauer spectra for $EuSn_2P_2$ at temperatures (T) = 15 K and 298 K.

In a future study, we will demonstrate quantitative analysis on element specific internal magnetic fields, spontaneous magnetic moments, isomer shifts, a portion of mixed valent state, and Debye temperature of $EuSn_2P_2$.

These future study will verify bulk properties on the possible magnetic topological conductors, $EuSn_2Pn_2$ (*Pn* = P, As), in which the Eu ions exhibit the Kondo lattices.

REFERENCES:

[1] M. Q. Arguilla, *et al.*, Inorg. Chem. Front. 4, 378 (2017).
[2] X. Gui, *et al.*, ACS cent. Sci. 5, 900 (2019).
[3] G. M. Pierantozzi, *et al.*, Proc. Natl. Acad. Sci. 119, e2116575119 (2022).
[4] R. Sakagami, *et al.*, Mater. Sci. Tech. Jpn. 55, 72 (2018) in Japanese.
[5] R. Sakagami, *et al.*, J. J. Appl. Phys. 60, 035511 (2021).
[6] R. Sakagami, Ph. D thesis, Keio University, 2021. Synthesis and transport properties of van der Waals-type quasi-two-dimensional pnictide, $EuSn_2As_2$
[7] Z. Klencsar: Mosswinn Program, Budapest, 2001 [http://www.mosswinn.com/].

PR7-11 Optimization for the energy standard material for Mössbauer spectroscopy

R. Masuda, S. Kitao[1], Y. Kobayashi[1], M. Kurokuzu[1], T. Fujihara[1], and M. Seto[1]

Graduate School of Science and Technology, Hirosaki University
[1]Institute for Integrated Radiation and Nuclear Science, Kyoto University

INTRODUCTION: Mössbauer spectroscopy is usually known as a powerful method for the analysis of iron compounds. In fact, most of Mössbauer experiments has been performed using ^{57}Fe nuclide, although the other nuclides are also available in Mössbauer spectroscopy, in principle. This is because there is a critical problem in the preparation of the γ-ray source; we can purchase ^{57}Co for γ-ray source of ^{57}Fe Mössbauer spectroscopy, but we cannot do the corresponding radioactive isotopes for γ-ray source for Mössbauer spectroscopy using various nuclide. This problem can be overcome by making the isotopes by a nuclear reactor or an accelerator. KURNS has all of them and is actually the most active research institute for Mössbauer spectroscopy using various nuclides.

Recently, we are focused on the Mössbauer spectroscopy using rare-earth nuclides. The 4*f* electrons causes various electronic states, such as Kondo state. One of nuclides available for Mössbauer spectroscopy is ^{151}Eu. Mössbauer spectroscopy using this nuclide is usually used performed with $^{151}SmF_3$ at room temperature because the recoilless fraction, the probability of Mössbauer effect, is reasonable at room temperature. However, recoilless fraction always increases as the temperature decreases. [1] Fig. 1 shows the temperature-dependence of the recoilless fraction of $^{151}EuF_3$, which is the decay product after the β-decay of $^{151}SmF_3$. The recoilless fraction is around 0.6 at room temperature, but it reaches around 0.9 at 10 K. This predicts further efficient measurement with 1.5 times deeper absorption by cooling the source material. However, there is another requisite; it should not have hyperfine splitting even at low temperature, although rare-earth element often shows magnetic order which induces nuclear Zeeman splitting and sometimes structural change from room temperature. Therefore, we measured Mössbauer spectra of EuF_3 at low temperature to certify no hyperfine splitting for the improvement of the efficiency of ^{151}Eu Mössbauer spectroscopy.

EXPERIMENTS: The sample was non-enriched EuF_3 purchased from Wako pure chemical industry. The sample was shaped to the pellet with the cross section of 20 mmφ and the thickness of 25.3 mg EuF_3/cm^2. The Mössbauer spectroscopy was performed at Tracer Laboratory at KURNS. The γ-ray source was $^{151}SmF_3$ and the transmitted γ-rays after the cooled EuF_3 sample was detected by Xe proportional counter.

RESULTS: Fig. 2 shows the ^{151}Eu Mössbauer spectra at some temperatures. No evidence of hyperfine structure is observed even at 10 K. Furthermore, the velocity values at absorption are equal in experimental error, about 0.05 mm/s for all temperatures. This is also reasonable even when we consider the second order Doppler shift, the thermal effect to the velocity value at absorption. The shift is calculated to be 0.057 mm/s at maximum in our case and similar to the experimental error. In the case of ^{151}Eu, the isomer shift, the effect of valence state, is quite larger than this error; the difference between the isomer shift of Eu^{3+} compounds and those of Eu^{2+} ones, are typically 10 mm/s. Therefore, we can discuss the valence without any special consideration of the effect of second order Doppler shift at EuF_3.

This result suggests that the efficiency of ^{151}Eu Mössbauer spectroscopy can be improved by cooling not only at Mössbauer spectroscopy with conventional radioactive γ-ray source, but also that with synchrotron radiation.

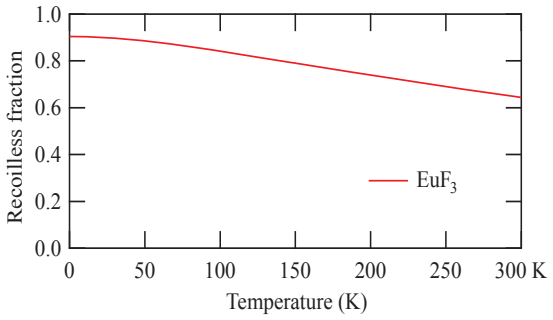

Fig. 1. Calculated Recoilless fraction of Mössbauer effect for ^{151}Eu nuclear resonance at EuF_3.

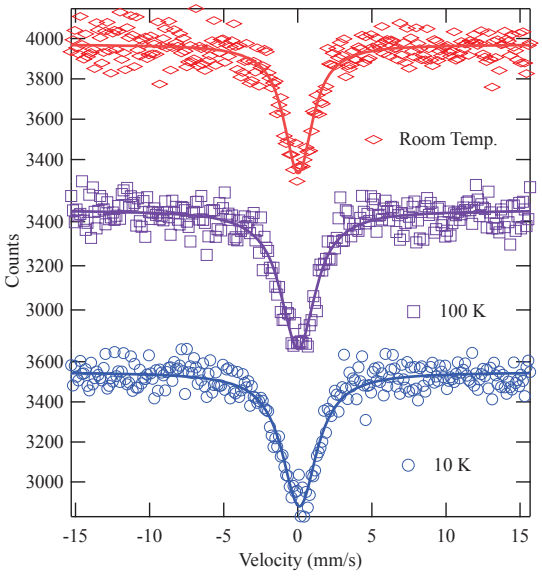

Fig. 2. ^{151}Eu Mössbauer spectra of EuF_3 at some temperatures.

REFERENCES:

[1] N. N. Greenwood and T. C. Gibb, Mössbauer Spectroscopy (Chapmann and Hall Ltd, London, 1971).

PR7-12 Development of ^{180}Hf Mössbauer Spectroscopy

S. Kitao[1], Y. Kobayashi[1], M. Kurokuzu[1], T. Kubota[2], H. Tajima[3], T. Fujihara[3], H. Yamashita[3], R. Masuda[4], and M. Seto[1]

[1]*Institute for Integrated Radiation and Nuclear Science, Kyoto University*

[2]*Agency for Health, Safety, and Environment, Kyoto University*

[3]*Graduate School of Science, Kyoto University*

[4]*Faculty of Science and Technology, Hirosaki University*

INTRODUCTION:

The Mössbauer spectroscopy is one of the most powerful methods to investigate electronic states and magnetic properties by extracting the information of a specific isotope. Even though more than one hundred of Mössbauer energy levels are known, Mössbauer spectroscopy in general is performed for quite limited isotopes, such as ^{57}Fe and ^{119}Sn. In order to promote studies for less-common Mössbauer isotopes, we have been developing practical methods for short-lived Mössbauer sources by neutron irradiation at Kyoto University Reactor (KUR). Moreover, some short-lived isotopes can be complementarily produced by high-energy γ-ray irradiation converted from electron beam using the electron linear accelerator (KURNS-LINAC). We have already developed practical preparation methods of the Mössbauer sources for various isotopes (source nuclides in parentheses): ^{61}Ni(^{61}Co), ^{125}Te(^{125m}Te), ^{129}I(^{129}Te,^{129m}Te), ^{161}Dy(^{161}Tb), ^{166}Er(^{166}Ho), ^{169}Tm(^{169}Er), ^{170}Yb(^{170}Tm), ^{197}Au(^{197}Pt), etc.

In this research, a new attempt for ^{180}Hf Mössbauer spectroscopy is described. Hf has several Mössbauer isotopes and energy levels: ^{176}Hf(88.36 keV), ^{177}Hf(112.97 keV), ^{178}Hf(93.2 keV), ^{180}Hf(93.33 keV). However, all of these levels have high γ-ray energy of about 100 keV and their parent isotopes have short half-lives[1]. Because of these disadvantages, Hf Mössbauer spectroscopy have not been studied actively so far. Hf is an important element for some industrial applications and material sciences. Therefore, the improvement of the methods for Hf Mössbauer spectroscopy is necessary to become a useful technique to investigate Hf compounds.

EXPERIMENTS AND RESULTS:

Among the Hf Mössbauer levels, an attempt for the 93.3 keV level of ^{180}Hf has been studied. By neutron irradiation of ^{179}Hf, ^{180m}Hf with a half-life of 5.5 hours is produced[2,3]. Since a natural Hf contains ^{179}Hf with an abundance of 13.6 %, natural Hf was used for this experiment. As a candidate of the single-line material, HfC is tried as a source material. HfC was pelletized with Al powder and rapped with Al foil for the neutron irradiation. The irradiation was performed at the pneumatic tube(Pn) of KUR for 4 hours at 1MW operation or 1 hour at 5MW. In order to reduce shorter lived by-product, the irradiated source has used after waiting for a few hours from the end of irradiation. Since the recoilless fraction of Mössbauer isotope with high-energy level is low at high temperature, the sample and the source are cooled at the temperature of about 22 K. The γ-rays with the energy of 93.3 keV have been measured by a $CeBr_3$ scintillation detector. The spectra were measured for about half a day. The observed Mössbauer spectrum of HfC absorber using HfC source is shown in Fig. 1. The Mössbauer absorption spectrum has been successfully observed. Since the line shape is almost single line, ^{180}Hf Mössbauer spectroscopy will be able to be performed to some extent.

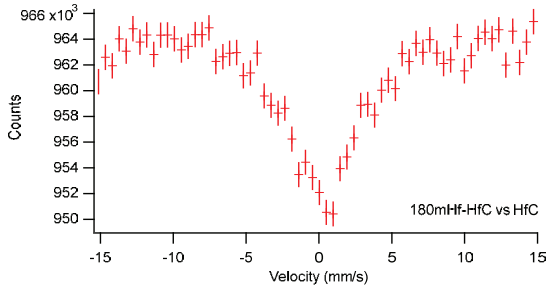

Fig. 1. ^{180}Hf-Mössbauer spectrum of HfC using ^{180m}Hf source in HfC at 22K.

Figure 2 shows Mössbauer spectrum of HfO_2 absorber using HfC source. The spectrum is apparently broader than HfC absorber due to the quadrupole splitting of HfO_2.

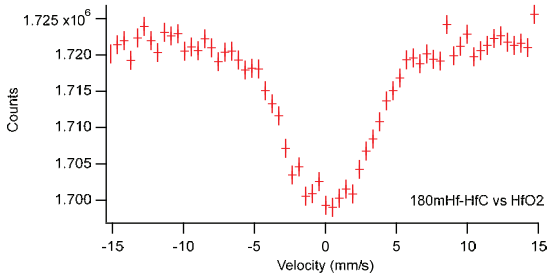

Fig. 2. ^{180}Hf-Mössbauer spectrum of HfO_2 using ^{180m}Hf source in HfC at 22K.

In summary, it is successfully confirmed that ^{180}Hf Mössbauer spectroscopy can be performed by a ^{180m}Hf source obtained by neutron irradiation of natural Hf. However, further improvement of the source material and measurement efficiency must be required for a practical spectroscopy.

REFERENCES:

[1] "Mössbauer Spectroscopy" N. N. Greenwood and T. C. Gibb (Chapman and Hall, London, 1971).

[2] E. Gerdau, H. J. Körner, J. Lerch, P. Steiner, Z. Naturforsch. **21 a**, 941(1966).

[3] R. E. Snyder, J. W. Ross, D. St P. Bunbury, J. Phys. C: Sol. Stat. Phys. **1**, 1662(1968).

PR7-13 Experimental Preliminary Approaoch on the Precipitation Mechanism of Banded Iron Formation (BIF)

K. Yonezu, H. Hirano[1], K. Hongo[1], Y. Kobayashi[2] and T. Yokoyama[3]

Department of Earth Resources Engineering, Faculty of Engineering, Kyushu University
[1]Department of Earth Resources Engineering, Graduate School of Engineering, Kyushu University.
[2]Institute for Integrated Radiation and Nuclear Science, Kyoto University
[3] Department of Chemistry, Faculty of Sciences, Kyushu University

INTRODUCTION: Banded Iron Formation (BIF) is chemically precipitated sedimentary rock at Precambrian age. Currently iron resource widely used in our industries largely depends on BIF. BIF was formed by seafloor hydrothermal activity. In addition, the hydrothermal water, anoxic water was mixed with oxic seawater (e.g., Otake and Otomo, 2021). However, there are many mysteries on the formation mechanism. One of the biggest issue is the alternation of iron mineral and silicate (+carbonate) minerals. Therefore, this study aims to understand the formation mechanism, especially redox condition during the formation of BIF.

EXPERIMENTS: The samples used here were collected from operating geothermal power plant or prepared by the rapid pH change of iron/silica bearing solutions. Former samples are so called silica scale, and those were analyzed by XRF and NMR. Latter samples were collected by filtration using 0.45μm and analyzed by mainly XRD. Precipitation percentage of iron and silica were also determined by ICP-AES using the difference before and after precipitation.

The precipitation experiments were carried out using the fixed volume (250ml) of aqueous solutions to limit the dissolved oxygen concentration. Once the dissolved oxygen was consumed to form iron bearing precipitates, no atmospheric oxygen affected in the system. Therefore, as increasing in ferrous ion in the system, more dissolved oxygen was consumed to create more anoxic condition during the experiments (reaction time was 15 minutes).

RESULTS: Five of silica scale samples were chemically analyzed. Those were directly precipitated from geothermal water, model of anoxic hydrothermal water without mixing by oxic aqueous solutions. Iron concentration in geothermal water is below detection limits of ICP-AES (less than 0.01 ppm), while iron concentration as Fe_2O_3 in silica scale were up to 15% (Tab. 1). This fact suggested that iron is specifically concentrated in silica scale. The concentration mechanism is still in discussion, but further Mossbauer spectroscopy strongly help understanding the precipitation mechanism due to amorphous form of silica scale. At least, some of aluminum precipitated as 6-coordination by NMR, suggesting that smectite group mineral precursor was formed.

Tab. 1. Chemical composition of silica scale used in this study.

	Unit	Sample 1	Sample 2	Sample 3	Sample 4	Sample 5
H2O(-)	%	0.0	5.4	2.5	3.8	0.9
H2O(+)	%	15.5	8.3	7.6	9.2	8.6
Fe2O3	%	0.2	12.0	12.3	4.8	15.6
Al2O3	%	12.9	7.0	6.6	10.5	9.3
Na2O	%	1.6	0.8	0.6	1.4	1.4
K2O	%	1.8	0.7	0.3	1.2	1.2
CaO	%	4.5	2.5	1.4	2.3	3.7
MgO	%	0.4	10.5	18.9	7.0	1.7
SiO2	%	75.3	55.6	49.1	70.2	67.3

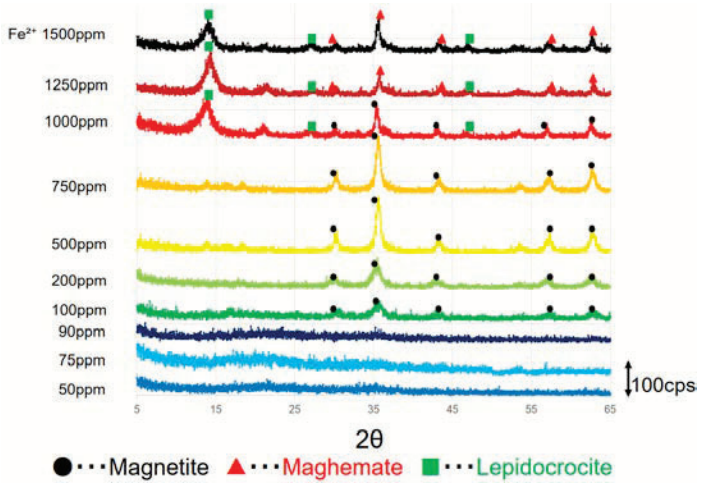

Fig. 1. XRD patterns of iron precipitates obtained from various initial ferrous concentration.

As shown in Fig. 1, different initial concentration of ferrous ion led to the different mineralogy of iron bearing precipitates. The monitored dissolved oxygen was almost zero when initial ferrous ion was more than 100 ppm. At the initial ferrous ion greater than 100 ppm, some of crystalized iron bearing minerals could be observed, while only amorphous phase precipitates (iron hydroxide) were collected less than 90 ppm initial ferrous ion conditions.

Crystalized iron bearing mineral can be further identified as magnetite, maghemite and lepidocrocite. Magnetite is dominant at 100-1000 ppm of initial ferrous ion, while maghemite is dominant at above 1250 ppm. In addition, lepidocrocite could be formed at above 1000 ppm of initial ferrous ion together with magnetite or maghemite. In order to fully understand the iron speciation of the precipitates, Mossbauer spectroscopy is powerful tool.

REFERENCES:

[1] T. Otake and Y. Otomo, Shigen-Chishitsu, **71** (2021) 57-73.